A diffusion model for solute atoms diffusing and aggregating in nuclear structural materials*

Quan Song(宋泉)[1,2], Fan-Xin Meng(孟繁新)[3], Bo-Yuan Ning(宁博元)[4], Jun Zhuang(庄军)[4], and Xi-Jing Ning(宁西京)[1,2,†]

[1] *Institute of Modern Physics, Fudan University, Shanghai* 200433, *China*
[2] *Applied Ion Beam Physics Laboratory, Fudan University, Shanghai* 200433, *China*
[3] *China ZhenHua Group YongGuang Electronics Co., Ltd. (State-owned* 873 *Factory), Guiyang* 550018, *China*
[4] *Department of Optical Science and Engineering, Fudan University, Shanghai* 200433, *China*

(Received 19 June 2017; revised manuscript received 13 September 2017; published online 20 November 2017)

In nuclear structural materials, the nuclear irradiations induce the precipitations of soluble elements or produce the insoluble elements such as He atoms that may form clusters, heavily shortening the service life-times of the materials. In the present work, a diffusion model is developed to predict where and how fast the solute atoms (either soluble or insoluble) aggregate, and this model is applied to the study of the formation and growth of He bubbles in metal tritides ($PdT_{0.6}$, ErT_2, $NbT_{0.0225}$, $VT_{0.5}$, $TaT_{0.097}$, $TiT_{1.5}$, $ZrT_{1.6}$) within one thousand days. The results are in good agreement with the available experimental observations and suggest that searching for metals with a barrier of more than 1.1 eV for a single He atom diffusion and making more defects in metal tritides can significantly reduce the growth of He bubbles and extend the service time of the metals.

Keywords: atomistic modeling, diffusion growth, metal tritides, nucleation and growth, helium bubble

PACS: 66.30.J–, 61.72.–y **DOI:** 10.1088/1674-1056/26/12/126601

1. Introduction

Because of the global pressing demands for energy, nuclear power stations such as Generation IV fission and fusion reactors are considered currently.[1] One of the most crucial issues is safety of the plants, which are expected to work for more than four decades.[2–5] This challenges researchers to design the structural materials that can withstand extreme stress, high temperature, and high irradiation dose. Some experimental studies on ferritic alloys have demonstrated that the long-termed irradiation results in precipitation of soluble elements such as Cu, Mn, Ni, Si, and P, dramatically leading to embrittlement,[6] and some insoluble elements such as He, generated from either (n, α) reaction or tritium (T) decay, can form clusters that may grow without bound.[4] Clearly, aggregation of solute atoms (either soluble or insoluble) will seriously shorten the service life-time of nuclear structural materials. Recently, some researchers reported that metal-graphene nano-layered composites display enhanced radiation resistance.[7,8] In order to develop novel materials of longer lifetime, it is highly desired to establish a dynamic model to predict where and how fast solute atoms aggregate in bulk materials to see what approaches are effective to reduce the aggregating rate.

This is a challenging issue[9] and a great many of experimental and theoretical efforts have been made to cope with this problem.[1,10–17] Extensive observations showed that crystal boundaries may lead to the solute atoms sinking in the materials[1,12,18,19] and that the defects (vacancies or dislocation) within the crystal grains also act as the aggregation traps.[4,20–22] Under nuclear irradiation, much more such defects can be produced and therefore, the solute atoms within crystal grains are more likely to be aggregated. In addition, when two solute atoms encounter within a crystal grain, they might form a dimer and further grasp other solute atoms to form interstitial clusters (self-trapping mechanism).[23] The problem is what are the probabilities (or rates) for these three kinds of nucleation mechanisms respectively. We cannot expect that atomic microscopy is a very effective approach to this problem because the aggregation involves with the atomic diffusion events only containing one or two solute atoms, which could hardly be observed directly even using the most advanced atom probe instruments. What is even worse is that the aggregation rates might be different during the service periods of more than several decades, so the experimental measurements would take too much time. Molecular dynamics simulation on atomic diffusion events seems to be a direct approach to the problem, but the efficiency is too low to simulate an aging process of bulk material in size larger than micrometers and lasting more than one microsecond.[24,25] Kinetic Monte Carlo (KMC) method proved to be very powerful for addressing this issue,[26,27] but when the hopping frequency of solute

*Project supported by the Specialized Research Fund for the Doctoral Program of Higher Education, China (Grant No. 20130071110018) and the National Natural Science Foundation of China (Grant No. 11274073).

†Corresponding author. E-mail: xjning@fudan.edu.cn

© 2017 Chinese Physical Society and IOP Publishing Ltd

atom is larger than 10^6 Hz, corresponding to the diffusion barrier smaller than about 0.45 eV, the method cannot describe evolution on a macroscopic time scale.

In the present work, we establish a diffusion equation to address the above problems. The diffusion coefficient was determined by a so-called single-atom statistical model,[28] which has been successfully used to predict atomic diffusion rate,[29,30] the stability of nanomaterials,[31–33] molecular reaction rates,[34,35] and other properties.[36] The diffusion equation was used to study the formation and growth of He cluster in metal tritides aged with time t, on which extensive experimental data have been accumulated[37–40] and a kinetic theoretical model has been developed.[40] Based on the mechanism of self-trapping (interstitial clustering), the model suggests that the density of He bubbles is mainly determined by the diffusion coefficient of single He atom and can explain some experimental observations. However, it is difficult to answer why the same kind of metal tritide exhibits different densities of He bubbles in different experiments.[41–43] (See Table 1 for details) and why the bubble densities are the same at both room temperature and low temperature (−196 °C).[44] Our theoretical results show that nucleation of He atoms in defects within crystal grains is the main mechanism for most of metal tritides, and the diameter of the He cluster increases linearly with $t^{1/3}$ at room temperature and reaches up to about 1.5 nm in about one hundred days, which is in good agreement with previous experimental observations.[9,37–39,41,42] Our calculations suggest that searching for metals with a barrier of more than 1.1 eV for single He atom diffusion in the metal or reducing the ambient temperature down to 200 K are two efficient ways to reduce the sizes of He bubbles for extending the service life-time.

Table 1. Lattice constants of some metal tritides, the diffusion barriers of single He atom, and the densities of He bubbles measured experimentally. For $PdT_{0.6}$, the measured diffusion coefficient, 0.2×10^{-16} $cm^2\cdot s^{-1}$–2×10^{-16} $cm^2\cdot s^{-1}$, is listed instead of the diffusion barrier.

Specimen	Bubble density/m^3	Diffusion barrier/eV	Lattice Parameter/Å
$PdT_{0.6}$[41]	5×10^{23}–10×10^{23}	0.2×10^{-16} $cm^2\cdot s^{-1}$–2×10^{-16} $cm^2\cdot s^{-1}$	4.033
$PdT_{0.6}$[42]	3×10^{24}–10×10^{24}		
$TiT_{1.5}$[38]	5×10^{23}	1	4.424
$ZrT_{1.6}$[39]	5×10^{23}	1	4
ErT_2[43]	0.97×10^{23}	0.49	5.125
	2.9×10^{23}		
	3.2×10^{23}		
	9.1×10^{23}		
$NbT_{0.0225}$[45]	5×10^{23}	0.66	2.86
$VT_{0.5}$[44]	3.5×10^{22}	0.08	3
$TaT_{0.097}$[45]	5×10^{22}	0.09	2.87

2. Models and methods

Firstly, we consider the aggregation events caused by defects within crystal grains in common bulk materials as shown in Fig. 1(a). Usually, the grain size is about tens of micrometers and the defects distribute homogenously within a crystal grain, i.e., any defect is surrounded by a volume in which the solute atoms exist and diffuse as shown in Fig. 1(b). On an average, a grain can be divided into many regions of the same volume with one defect located in the center, and for simplicity, each defect is considered to be a small ball of radius r_0 located in the center of a large ball of radius R as shown in Fig. 1(c). The density of solute atoms outside the defect,$\rho(r,t)$, obeys diffusion equation

$$\frac{\partial\rho(r,t)}{\partial t}-\frac{D}{r^2}\frac{\partial}{\partial r}\left(r^2\frac{\partial\rho(r,t)}{\partial r}\right)=G(r,t),\quad(r_0<r<R),\ (1)$$

where D is the diffusion coefficient of the solute atoms, and $G(r,t)$ the rate of solute atoms produced per unit volume. For soluble elements such as Cu, Mn or Ni, which are the components of structural materials, $G(r,t)=0$, while for insoluble atoms such as He atoms, continuously produced by nuclear irradiation or decay, $G(r,t)\neq0$. Assuming that a defect can trap any solute atom once it enters into the defect, the inner boundary condition for Eq. (1) is $\rho(r_0)=0$, and the total number of solute atoms at aging time t trapped by the defect is $N(t)=4\pi r_0^2 D\int_0^t\nabla_r\rho(r,\tau)|_{r=r_0}\,\mathrm{d}\tau$. The boundary condition at $r=R$ is taken as $\nabla\rho|_{r=R}=0$, reflecting the fact that the spatial distribution of the solute atoms is homogeneous in the area far from the defect.

Secondly, we consider the interstitial clustering of solute atoms wondering in crystal lattices. Generally, a single solute atom in a bulk material can migrate and may encounter with another solute atom to form a dimer that stays at an interstitial site within a perfect lattice and may further grasp other solute atoms.[23] On an average, any single solute atom can be regarded as a spherical defect with a radius equal to the distance between two solute atoms that form a dimer, so in the same way as that for the defect, equation (1) is applicable to calculating the number of solute atoms grasped by a given single

solute atom as long as the radius r_0 is considered to be increasing with the number of solute atoms increasing in the clusters, i.e., $r_0 = \left[3N(t)/4\pi\rho_{\text{guest}}\right]^{1/3}$ mathematically, where ρ_{guest} is the density of the solute atoms in the cluster. Obviously, the aggregation of solute atoms in grain boundary, S, can also be described by Eq. (1) as long as the boundary condition is taken as $\rho(R) = 0$.

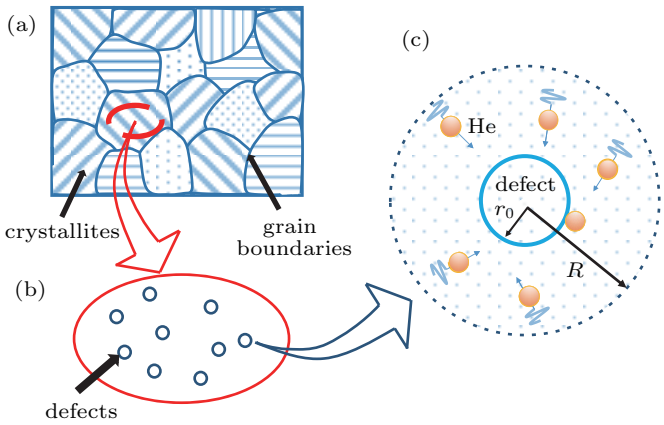


Fig. 1. (color online) Schematic diagrams of bulk materials composed of (a) crystal grains and (b) defects (circles) in a crystal grain. For simplicity, a defect is considered to be a small ball of radius r_0 located in the center of a big ball of radius R, in which there may exist solute atoms (c).

The key quantity in Eq. (1) is the diffusion coefficient $D = \Gamma L^2/6$, where Γ is the frequency for a solute atom escaping from a potential well $V(x)$ with width L (Fig. 2) and can be obtained via the single-atom statistical model:[28,29]

$$\Gamma = \frac{\Gamma_0}{Z}\int_{E_0}^{\infty} \varepsilon^{1/2} \mathrm{e}^{-\varepsilon/k_{\mathrm{B}}T}\,\mathrm{d}\varepsilon, \tag{2}$$

where $Z = \sqrt{\pi}(k_{\mathrm{B}}T)^{3/2}/2$ is the partition function and Γ_0 reads

$$\Gamma_0 = \frac{\int_0^{E_0} \nu\varepsilon^{1/2} \mathrm{e}^{-\varepsilon/k_{\mathrm{B}}T}\,\mathrm{d}\varepsilon}{\int_0^{E_0} \varepsilon^{1/2} \mathrm{e}^{-\varepsilon/k_{\mathrm{B}}T}\,\mathrm{d}\varepsilon}, \tag{3}$$

where

$$\nu = \left\{4\sqrt{m}\int \mathrm{d}x/\sqrt{2\left[\varepsilon - V(x)\right]}\right\}^{-1}.$$

To apply this model to bulk materials, we need to calculate the potential curve, $V(x)$, along the lowest energy migration path, which can be implemented by first-principle calculations. If the barrier E_0 is determined experimentally, $V(x)$ can also be obtained by a sine function fitting.

3. Results and discussion

Up to the present, many efforts have been dedicated to exploring the nucleation mechanism of the He bubbles in bulk material. For the bubbles in aging metal tritides, self-trapping (interstitial clustering) of the He atoms were considered to be the main mechanism[23,38–40] and several kinetic models have been developed. Based on this mechanism,[40] the bubble nucleation occurred during the first few days, followed by implantation of tritium into the metals and later the newly born He atoms aggregated at these nucleation sites rather than formed new ones, which can explain the experimental observations that the density of He bubbles within crystal grains kept unchanged during the aging in one hundred days.[42] The calculations from the model[40] showed that the bubble density is sensitive to the He diffusivity. Thus, for metal tritides of the same chemical components, the density of He bubbles within the crystal grains should be the same no matter what the specific specimen is, while for metal tritides of different chemical components, the bubble densities should be different. However, the bubble densities in Pd tritides, measured by different groups may differ by about ten times, such as $5-10\times10^{17}/\mathrm{cm}^3$ reported in Ref. [41] and $3-10\times10^{18}/\mathrm{cm}^3$ in Ref. [42], and the density observed in ErT_2 ranges from $0.97\times10^{17}/\mathrm{cm}^3$ to $9.1\times10^{17}/\mathrm{cm}^3$ (See Table 1), corresponding to different thickness values of the sample. Vanadium tritides observed at room temperature and at low temperature ($-196\,^{\circ}\mathrm{C}$) in the same experiment[44] exhibited the same density of He bubbles ($3.5\times10^{17}/\mathrm{cm}^3$), which obviously contradicts the self-trapping mechanism because diffusivity of the He atoms greatly decreases at the low temperature.

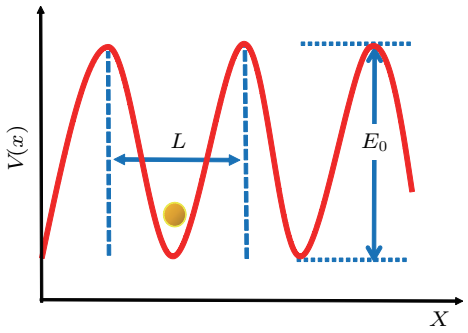


Fig. 2. (color online) Schematic diagram of a solute atom of kinetic energy ε confined in a potential well $V(x)$ with width L.

Our diffusion models have been used to study the dynamics of He bubble growth in metal tritides, $PdT_{0.6}$,[41] Pd-based alloys,[42] ErT_2,[43] $NbT_{0.0225}$,[45] $VT_{0.5}$,[44] $TaT_{0.097}$,[45] $TiT_{1.5}$,[38] and $ZrT_{1.6}$,[39] on which the time dependence of the bubble size was measured (See Table 1). The realistic metal tritide consists of crystal grains, and there may exist defects (vacancies or impurities) within the grain. Assuming that the defects are distributed homogenously within the crystal grains and He atoms decayed from tritium are only trapped by the defect without interstitial clustering, we calculate the He bubble size at the defect as a function of aging time t. Thus, the density of He bubbles, which is found to be unchanged with the aging time in nearly all the relevant experiments, should be the density of the defects, ρ_{D}, and a defect is surrounded by a big ball with a radius of $R = (3/4\pi\rho_{\mathrm{D}})^{1/3}$. In early experiments the defects were rarely observed, so we assumed that they are small balls with a radius $r_0 = 0.5$ nm.[39] The production rate of the He atoms from tritium decay is $G(r,t) = n_0\alpha\,\mathrm{e}^{-\alpha t}$

($r_0 < r < R$), where α is the decay constant ($1.78 \times 10^{-9} s^{-1}$), and n_0 the original density of the T atoms. For calculating the diffusion coefficient ($D = \Gamma L^2/6$) of single He atom, the measured diffusion barrier E_0 is employed in Eqs. (2) and (3) to determine Γ, and the width of the diffusion barrier L is considered to be half of the lattice constant. Because most of metal tritides are fcc structures and the two nearest tetrahedral sites, which are the positions of the energy minimum for single He atom to occupy, their distance is half of the lattice constant. Assuming the bubble to be spherical, the diameter d is obtained via $d = (6N/\pi\rho_{He})^{1/3}$, where ρ_{He} is the density of the He atoms in the bubble, determined in previous experiments.[39] Employing the parameters listed in Table 1, the calculation results are shown in Fig. 3 and listed in Table 2.

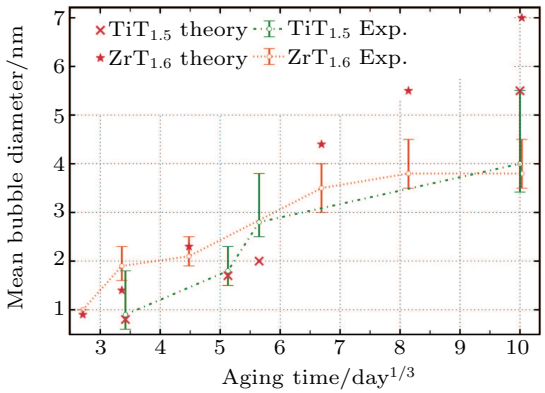


Fig. 3. (color online) Variations of sizes of the He bubble calculated with our model and observed on $TiT_{1.5}$ and $ZrT_{1.6}$ with aging time t.

When the above results are compared with the experimental measurements, it should be pointed out that the sizes of various He bubbles formed in metal tritides are not the same, but distributed in certain ranges and therefore the measured size and density of He bubbles are the average results. On the He bubble growth in bulk $PdT_{0.6}$,[41] the density of He bubbles, measured in one experiment is $5 \times 10^{17}/cm^3$–$10 \times 10^{17}/cm^3$,[41] while in another experiment is $3 \times 10^{18}/cm^3$–$10 \times 10^{18}/cm^3$.[42] The calculations using a diffusion coefficient of 0.2×10^{-16} $cm^2 \cdot s^{-1}$–2×10^{-16} $cm^2 \cdot s^{-1}$ in Eq. (1) show that when the density is $5 - 10 \times 10^{17}/cm^3$, the diameter of He bubble is about 1.7 nm–2.2 nm in 66 aging days, while for density of $3 - 10 \times 10^{18}/cm^3$, the corresponding diameter is about 0.8 nm–1.2 nm in 60 aging days (see Table 2), which are in good agreement with the corresponding experimental measurements, 1.5 nm∼2 nm[41] and 1 nm,[42] respectively. If the smallest limit of the measured diffusion coefficient, 0.2×10^{-16} $cm^2 \cdot s^{-1}$, is used in Eq. (1), the calculations show that in long-termed aging (longer than two months), all the generated He atoms are trapped by the defect, while in short-termed aging (about ten days), about 10 at.%∼20 at.% (or 20 at.%∼40at.%) of the He atoms stagnate in the matrix in 20 days (or 7 days). This result can explain the experimental observations[41] that in 7 or 20 aging days no He bubbles were detected in $PdT_{0.6}$ at room temperature while small He bubbles appeared when the samples were heated up to 600 K.

Table 2. Sizes of He bubbles measured in some metal tritides and calculated with our model.

Specimen	Measured bubble size/nm in (n) days	Calculated bubble size/nm in (n) days
$PdT_{0.6}$[41]	1.7–2.2 (66)	1.5–2(66)
$PdT_{0.6}$[42]	1 (60)	0.8–1.2 (60)
ErT_2[43]	15.4±7.2 (400)	8.1 (400)
	8.3±0.9 (350)	5.4 (350)
	12.3±4.9 (320)	5.1 (320)
	3.6±0.8 (350)	3.7 (350)
$NbT_{0.0225}$[45]	1.7 (600)	1.6 (600)
$VT_{0.5}$[44]	1–2 (80)	1.7 (80)
$TaT_{0.097}$[45]	5.6 (600)	5.7 (600)

On the samples of $NbT_{0.0225}$, $TaT_{0.097}$, the measured bubble sizes are 1.7 nm and 5.6 nm in about 20 months,[45] respectively, and for $VT_{0.5}$, the measured bubble size in 80 days is 1 nm–2 nm,[44] which are in good agreement with our calculations, 1.6, 5.7, and 1.7 nm for each of the cases (see Table 2).

On ErT_2 thin films,[43,46] the observed densities of He bubbles are $0.97 \times 10^{17}/cm^3$, $2.9 \times 10^{17}/cm^3$, $3.2 \times 10^{17}/cm^3$, and $9.1 \times 10^{17}/cm^3$, corresponding to thickness values of the films 300, 500, 200, 100 nm,[43] respectively, and the corresponding measured bubble sizes are 15.4±7.2, 8.3±0.9, 12.3±4.9, and 3.6±0.8 nm in about 400, 350, 320, 350 days. Our calculations of these conditions show that the corresponding bubble sizes are 8.1, 5.4, 5.1, 3.7 nm (see Table 2), which are significantly smaller than the measured ones. This difference should be attributed to the fact that the bubble is assumed to be spherical bubble in our model, while the bubble shape observed in the experiment is platelet when the number ratio of He to metal atoms is less than 0.15, which is significantly larger than the ratio (< 0.05) in our calculation.

In the experiment of He bubble growth in titanium, the measured barrier for the He atom diffusion is 1±0.3 eV[47] and the measured density of He bubble is $5 \times 10^{17}/cm^3$.[38] If the barrier of 1.0 eV is employed, equation (1) shows that the bubble diameters aging at 300 K in 40, 135, 180, and 1000 days are 1.2, 2.5, 2.9, and 6.3 nm, respectively, which are larger than the measured sizes of 0.9, 1.8, 2.8, and 4 nm.[38] If the diffusion barrier is adjusted to 1.03 eV, the calculated diameters are 0.8, 1.7, 2.0, and 5.5 nm for the corresponding aging time. Within 180 days, the agreement is good, while for longer aging time, the calculated bubble size is larger than the measured one. Similar situations existed in $ZrT_{1.6}$.[39] The measured He bubble sizes in about 20, 40, 90, 300, 1000 days were about 1, 1.9, 2.1, 3.5, 3.8, 3.8 nm, respectively, while our calculated ones are 0.9, 1.4, 2.2, 4.4, 5.5, and 7.0 nm. Within 100 days, the calculated bubble sizes are in good agreement with the measured ones, while after 300 aging days, the calculation results are significantly larger. This disagreement may

be understood as follows. The diffusion or barriers employed in our calculations are measured at the beginning of metal tritides aging when a few tritium atoms decay and the born He atoms diffuse interstitially. After aging about one year, more tritium atoms decay and the formation of He bubbles could lead to dislocations and voids, hindering the He atoms from diffusing and therefore reducing the diffusion coefficient. Thus the bubble growth is more slowly than our predictions.

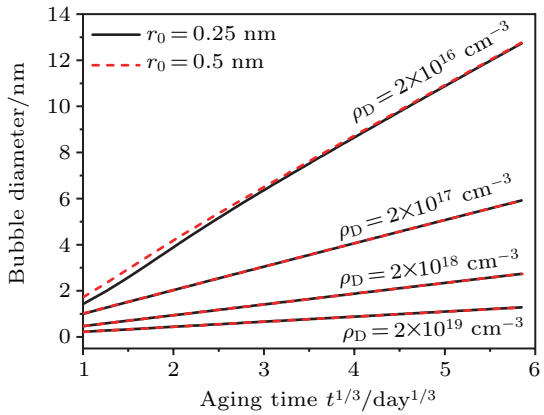


Fig. 4. (color online) Variations of calculated diameters of He bubbles formed at 300 K with aging time t for different defect densities with a diffusion barrier of 0.8 eV for $r_0 = 0.25$ nm and 0.5 nm within 200 days.

For a general understanding of the He behavior in metal tritides, we examine the influences of defect size and density ρ_D on He bubble growth within a crystal grain as shown in Fig. 1(c). Usually, the number ratio of T atoms to the metal atoms M ranges from 0.1 to 2 and we assume the ratio M: T to be 1. The lattice constants of most metal tritides are about 3 Å∼4 Å, such as 4.4 Å for TiT_2.[48], 4.0 Å for δ-ZrT,[49] 4.0 Å for $PdT_{0.67}$[40] and 2.9 Å for Nb and Ta tritides,[45] Thus, in our calculations the lattice constant is assumed to be 3.5 Å. Applying the above data and different diffusion barriers to the diffusion equation, we obtain the size of He cluster in the defect with $r_0 = 0.25$ nm (or $r_0 = 0.5$ nm) as a function of aging time within 200 days (see Fig. 4) at room temperature for the cases of $\rho_D = 2\times10^{16}$, 2×10^{17}, 2×10^{18}, and 2×10^{19}/cm^3. It is shown in Fig. 4 that when the diffusion barrier is 0.8 eV the defect density increases by three orders of magnitude while the bubble size decreases by ten times, and the bubble diameters for a given aging time t are almost the same when the defect radius changes from 0.25 nm up to 0.5 nm. In all the cases, the bubble size increases linearly with $t^{1/3}$. When the diffusion barrier increases from 0.8 eV up to 1.0 eV, the bubble size decreases by about three times for $\rho_D < 2\times10^{18}$/cm^3 (Fig. 5), while for other ρ_D the bubble size remains nearly unchanged. It is notable that if the barrier increases further by only 0.1 eV, i.e., $E_0 = 1.1$ eV, the bubble size for $\rho_D \le 2\times10^{18}$/cm^3 decreases by about ten times. Without changing the diffusion barrier (0.8 eV) but reducing the temperature down to 225 K (or 200 K), the bubbles also become significantly smaller (Fig. 6). In these cases, larger defects trap a little more He atoms than the smaller ones, while the relationship that the bubble size increases linearly with $t^{1/3}$ keeps nearly unchanged for the aging time t longer than one month.

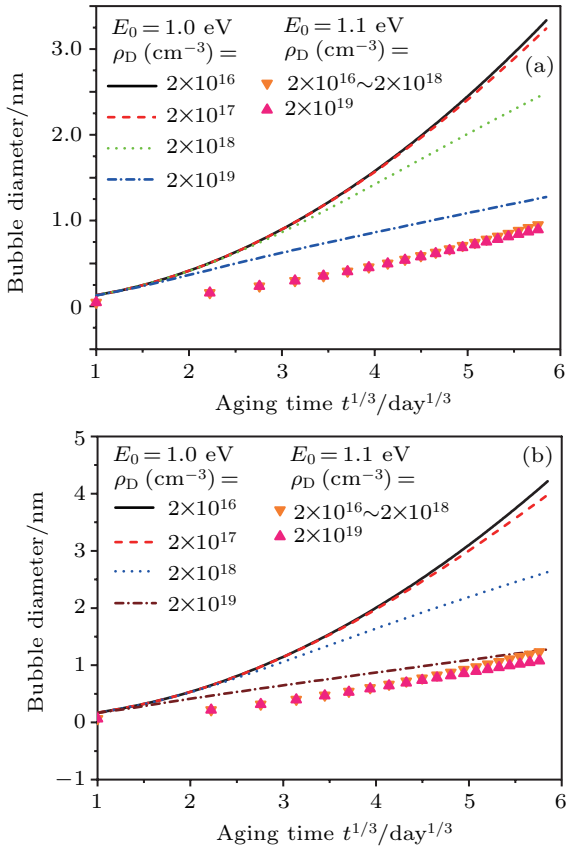


Fig. 5. (color online) Plots of calculated diameters of He bubbles formed at 300 K versus aging time t when the diffusion barrier increases from 0.8 eV up to 1.0 eV and 1.1 eV for (a) $r_0 = 0.25$ nm and (b) 0.5 nm.

For considering the probability for grain boundary trapping the He atoms, we continue to carry out the calculation with $E_0 = 0.8$ eV on a spherical crystal grain with a volume of 10 μm^3 containing only one defect with a radius of 0.25 nm (or 0.5 nm) in the center. As shown in Fig. 7(a), the number of He atoms trapped by the defect is about 0.01% of the one trapped by the boundary. Based on these data, if the defect density is 2×10^{17}/cm^3 or larger, the He atoms trapped by all the 2×10^6 defects within the crystal grains is more than about 100 time than those trapped by the boundary. For considering the probability for the He atoms to cluster interstitially within a crystal grain, we continue the calculations without any defect inside the crystal grain to see the density of He atoms within the grain. The calculations show that the densities of He atoms in the center region of the grain ball are all about 0.06 nm^{-3} for the diffusion barriers of 0.8, 0.9, and 1.0 eV after aging of 5 days (Fig. 7(b)), i.e., there exists only one He atom in a cubic box with a side length of about 25 Å, and the density near the boundary region is even smaller. If the diffusion barrier decreases down to 0.5 eV, the density decreases down to ∼10^{-5} nm^{-3}, i.e., there exists only one He atom in a cubic

box with a side length of 46 Å. This density of He atoms is too low for two He atoms to form a dimer or trimer because the formation energy of a dimer or trimer in metal tritide is significantly larger than that of an isolated He atom, such as in the case of Ti.[50] Certainly, the cluster of more than 5 or 6 He atoms, which can produce a vacancy in the crystal grain to form a nucleation center,[23] could hardly appear because the probability for 5 or 6 He atoms to encounter with each other simultaneously is too small for the He atoms at such a small density. This result indicates that most of the He atoms will be trapped in grain boundary if there are no lots of pre-existed defects within crystal grains.

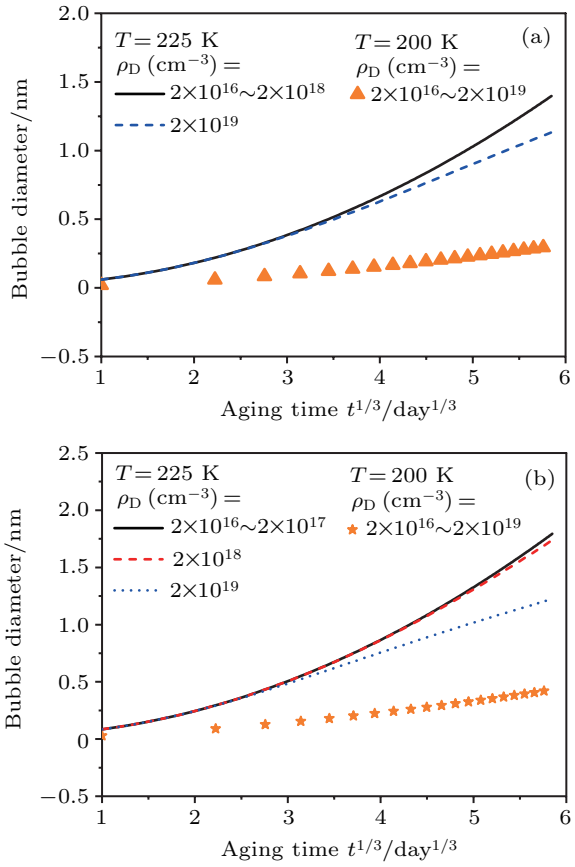


Fig. 6. (color online) Plots of diameters of He bubbles formed at 200 K and 225 K versus aging time t with a diffusion barrier of 0.8 eV for (a) $r_0 = 0.25$ nm and (b) 0.5 nm.

The above theoretical results are in good agreement with previous experimental observations and strongly suggest that defect trapping is the main mechanism for He atoms clustering instead of the self-trapping in metal tritides. First of all, the sizes of He bubble observed in most of experiments increase linearly with $t^{1/3}$,[38,39] which is in good agreement with our calculations (Figs. 4 and 5). And the bubble sizes observed after about two months, such as in experiments on $PdT_{0.6}$, Pd-based tritides, $VT_{0.5}$, $TiT_{1.5}$, and $ZrT_{1.6}$ (see Table 2 and Fig. 3), are about 1 nm–2 nm, which is not sensitive to the observed bubble density ranging from $3.5 \times 10^{17}/\mathrm{cm}^3$ to $10 \times 10^{18}/\mathrm{cm}^3$. These observations also coincide with our calculations shown in Figs. 4 and 5. Secondly, the observed He bubbles mainly appear within crystal grains instead of the grain boundaries, which coincides with our calculation that most of the He atoms are trapped by the defects with a density of larger than $2 \times 10^{17}/\mathrm{cm}^3$. If there are no pre-existing defects in crystal grain, our calculations show that the grain boundaries will trap lots of He atoms. Thirdly, the mechanism of defect trapping means that the density of He bubbles depends on the density of pre-existing defects rather than the diffusion coefficient of a single He atom, which can explain the experimental observations that the same kind of metal tritides may produce significantly different He bubble densities in different experiments — the densities of defects may be different in different processes of preparing the samples.

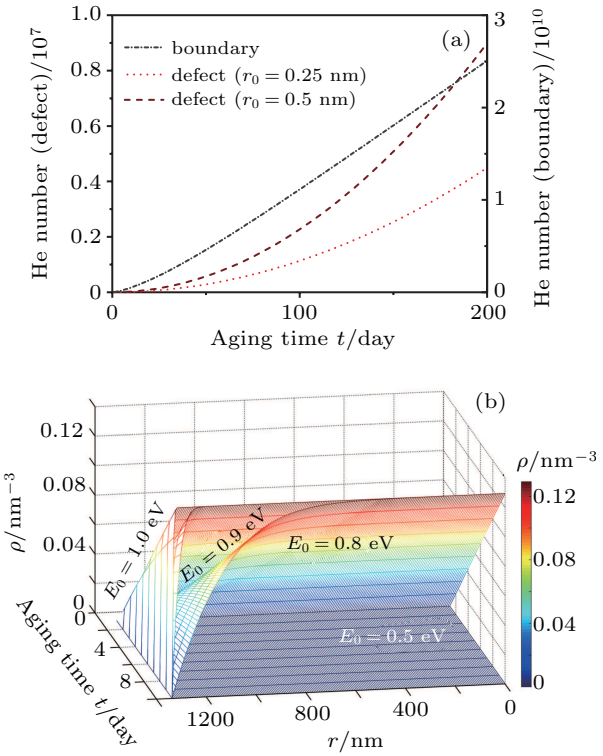


Fig. 7. (color online) (a) Calculated number of He atoms trapped by the boundary of a 10-$\mu\mathrm{m}^3$ grain ball in metal tritides with ratio M:T = 1 (short dash dotted line, right Y axis) and by a defect located in the center of the grain (dotted line for $r_0 = 0.25$ nm and dashed line for $r_0 = 0.5$ nm, left Y axis) as a function of aging time t (a); and (b) calculated density of He atoms within the crystal ball as a function of aging time t and the radius for different diffusion barriers: 0.5, 0.8, 0.9, and 1.0 eV.

The main argument supporting the self-trapping mechanism is that there exist few defects in crystal grains of the bulk metal to be tritided and no detectable defects in no-aged metal tritides.[41,44] Our calculations are based on the assumption that the defect sizes are only 0.5 nm∼1 nm, which may be too small to be detected by early TEM instruments. In fact, the studies of metal hydrides have shown that the hydride (or tritide) process inevitably produces lattice defects.[51,52] In the experiments of Ti–T system,[38] the authors suggested that there might exist 'denuded regions at high concentrations of

submicroscopic sizes (< 1 nm), which should be one kind of defect that can grasp He atoms.

4. Summary

We develop a diffusion model for describing the aggregation of solute atoms on macro-size and time scale in nuclear structural materials. Based on the model, the calculations of He bubble growth in most metal tritides show that the He atoms are mainly trapped by inherent defects within grains instead of self-trapping interstitials and the size of He bubble increases linearly with $t^{1/3}$ for most of metal tritides. Based on the calculations, three possible ways may be adopted to restrain the bubble size. Firstly, searching for metals with barriers of more than 1.1 eV for He atoms diffusing in the materials may be the most effective way, and secondly, reducing the ambient temperature down to 200 K is also an approach. Finally, making much more defects in materials may be a more reliable way nano-technology has achieved great developments. In conclusion, the diffusion model would find its vast applications in the near future.

References

[1] Marquis E A, Hyde J M, Saxey D W, Lozano-Perez S, de Castro V, Hudson D, Williams C A, Humphry-Baker S and Smith G D W 2009 *Mater. Today* **12** 30

[2] Bringa E M, Monk J D, Caro A, Misra A, Zepeda-Ruiz L, Duchaineau M, Abraham F, Nastasi M, Picraux S T, Wang Y Q and Farkas D 2012 *Nano. Lett.* **12** 3351

[3] Demkowicz M J, Hoagland R G and Hirth J P 2008 *Phys. Rev. Lett.* **100** 136102

[4] Beyerlein I J, Caro A, Demkowicz M J, Mara N A, Misra A and Uberuaga B P 2013 *Mater. Today* **16** 443

[5] Zinkle S J and Busby J T 2009 *Mater. Today* **12** 12

[6] English C A and Hyde J M 2003 6.08 — *Radiation Embrittlement of Reactor Pressure Vessel Steels*, in: I.M.O.R. Karihaloo (ed.), *Comprehensive Structural Integrity* (Oxford: Pergamon) pp. 351–398

[7] Huang H, Tang X B, Chen F D, Liu J and Chen D 2017 *J. Nucl. Mater.* **493** 322

[8] Kim Y, Baek J, Kim S, Kim S, Ryu S, Jeon S and Han S M 2016 *Sci. Rep.* **6** 24785

[9] Bond G M, Browning J F and Snow C S 2010 *J. Appl. Phys.* **107** 083514

[10] Nagai Y, Tang Z, Hassegawa M, Kanai T and Saneyasu M 2001 *Phys. Rev. B* **63** 134110

[11] Meslin E, Radiguet B and Loyer-Prost M 2013 *Acta Mater.* **61** 6246

[12] Jiao Z and Was G S 2011 *Acta Mater.* **59** 1220

[13] Birtcher R C, Donnelly S E and Templier C 1994 *Phys. Rev. B* **50** 764

[14] Knapp J A, Browning J F and Bond G M 2010 *Nucl. Instrum. Method B* **268** 2141

[15] Zhou Y L, Deng A H, Li R S, Zhang B L and Hou Q 2011 *Acta Phys. Sin.* **60** 046604 (in Chinese)

[16] Zhou H B and Jin S 2013 *Chin. Phys. B* **22** 76104

[17] Cheng G J, Fu B Q, Hou Q, Zhou X S and Wang J 2016 *Chin. Phys. B* **25** 76602

[18] Lane P L and Goodhew P J 1983 *Philos. Mag. A* **48** 965

[19] Han W Z, Demkowicz M J, Mara N A, Fu E, Sinha S, Rollett A D, Wang Y Q, Carpenter J S, Beyerlein I J and Misra A 2013 *Adv. Mater.* **25** 6975

[20] Blaschko O, Pleschiutschnig J, Glas R and Weinzierl P 1991 *Phys. Rev. B* **44** 9164

[21] Prem M, Krexner G and Pleschiutschnig J 2003 *J. Alloys Compd.* **356** 683

[22] Hua J, Liu Y L, Li H S, Zhao M W and Liu X D 2016 *Chin. Phys. B* **25** 36104

[23] Wilson W D, Bisson C L and Baskes M I 1981 *Phys. Rev. B* **24** 5616

[24] Zhang Y F, Millett P C, Tonks M, Zhang L Z and Biner B 2012 *J. Phys.-Condes. Matter* **24** 305005

[25] Morishita K, Sugano R and Wirth B D 2003 *J. Nucl. Mater.* **323** 243

[26] Domain C, Becquart C S and Malerba L 2004 *J. Nucl. Mater.* **335** 121

[27] Becquart C S and Domain C 2009 *J. Nucl. Mater.* **385** 223

[28] Lin Z Z, Yu W F, Wang Y and Ning X J 2011 *Europhys. Lett.* **94** 40002

[29] Yu W F, Lin Z Z and Ning X J 2013 *Chin. Phys. B* **22** 116802

[30] Yu W F, Lin Z Z and Ning X J 2013 *Phys. Rev. E* **87** 062311

[31] Xu Y G, Ming C, Lin Z Z, Meng F X, Zhuang J and Ning X J 2014 *Carbon* **73** 283

[32] Lin Z Z and Chen X 2013 *Europhys. Lett.* **101** 48002

[33] Ming C, Lin Z Z, Cao R G, Yu W F and Ning X J 2012 *Carbon* **50** 2651

[34] Lin Z Z, Li W Y and Ning X J 2014 *Chin. Phys. B* **23** 050501

[35] Li W Y, Lin Z Z, Xu J J and Ning X J 2012 *Chin. Phys. Lett.* **29** 080504

[36] Li J T, Wang J L, Zhang B Q, Rong X M and Ning X J 2014 *Acta Phys. Sin.* **63** 028101 (in Chinese)

[37] Beavis L C and Miglioni C J 1972 *J. Less-Common. Metals* **27** 201

[38] Schober T and Farrell K 1989 *J. Nucl. Mater.* **168** 171

[39] Schober T, Trinkaus H and Lasser R 1986 *J. Nucl. Mater.* **141–143** 453

[40] Cowgill D F 2004 *Sandia National Laboratories*, p. 42

[41] Thomas G J and Mintz J M 1983 *J. Nucl. Mater.* **116** 336

[42] Thiebaut S, Decamps B, Penisson J M, Limacher B and Guegan A P 2000 *J. Nucl. Mater.* **277** 217

[43] Snow C S, Brewer L N, Gelles D S, Rodriguez M A, Kotula P G, Banks J C, Mangan M A and Browning J F 2008 *J. Nucl. Mater.* **374** 147

[44] Schober T, Lasser R, Jager W and Thomas G J 1984 *J. Nucl. Mater.* **122** 571

[45] Schober T, Dieker C and Trinkaus H 1989 *J. Appl. Phys.* **65** 117

[46] Snow C S, Browning J F, Bond G M, Rodriguez M A and Knapp J A 2014 *J. Nucl. Mater.* **453** 296

[47] Vassen R, Trinkaus H and Jung P 1991 *J. Nucl. Mater.* **183** 1

[48] Quijano R, de Coss R and Singh D J 2009 *Phys. Rev. B* **80** 184103

[49] Schober T and Lasser R 1984 *J. Nucl. Mater.* **120** 137

[50] Liang J H, Dai Y Y, Yang L, Peng S M, Fan K M, Long X G, Zhou X S, Zu X T and Gao F 2013 *Comp. Mater. Sci.* **69** 107

[51] Schlapbach L 1988 *Hydrogen in Intermetallic Compounds I* (Springer)

[52] Berube V, Radtke G, Dresselhaus M and Chen G 2007 *Int. J. Energy Res.* **31** 637